

ANALYSIS OF RADIAL MAGNETIZED PERMANENT MAGNET BEARING CHARACTERISTICS

Siddappa I. Bekinal^{1,*}, Tumkur R. Anil¹,
and Soumendu Jana²

¹Department of Mechanical Engineering, Gogte Institute of Technology, Belgaum 590008, India

²Propulsion Division, National Aerospace Laboratories, Bangalore 560017, India

Abstract—With an increase in the number of high speed applications, researchers have been concentrating on permanent magnet bearings due to their suitability. This paper presents a mathematical model of a permanent magnet bearing made of ring magnets with radial polarizations. Coulombian model and vector approach are used to estimate the force, moment and stiffness. A MATLAB code is developed for evaluating the envisaged parameters for three degrees (translational) of freedom of the rotor. Comparison of force and stiffness results of the presented model with that reported in the literature and also with the results of 3D finite element analysis shows good agreement. Then, it is extended to analyse stacked ring magnets with alternate radial polarizations. Finally, the cross coupled stiffness values in addition to the principal stiffness values are presented for the elementary structure and also for stacked structure with three ring permanent magnets with alternate radial polarizations.

1. INTRODUCTION

Permanent magnet bearings are magneto-mechanical elements wherein the supporting property of bearing is realized by virtue of attractive or repulsive forces generated between the magnets. These are realized with ring magnets, axially, radially or perpendicularly magnetized. The force (bearing load) and stiffness are the important parameters to be considered in the design of permanent magnet bearings. The early work carried out towards the analysis of these parameters (two

Received 20 October 2012, Accepted 12 December 2012, Scheduled 19 December 2012

* Corresponding author: Siddappa Iranna Bekinal (sibekinal@git.edu).

dimensional analytical equations for force and stiffness) and synthesis of different configurations of permanent magnet bearings was by Yonnet [1, 2] and Delamare et al. [3]. The permanent magnet bearings are used in many applications like flywheels, turbo molecular pumps, turbomachines, artificial hearts and conveyor systems due to their suitable characteristics (high speed, lower wear, energy savings and freedom from lubricants) [4–7]. The stiffness of bearings made of two concentric rings is low, rings are arranged in a specific pattern to increase stiffness [8]. The force and stiffness of permanent magnet bearings are optimized by considering the effect of the number of parameters (number of rings, magnet volume, magnetization pattern and axial offset). The designer can use analytical approach, finite element analysis and experimental design methods for optimization. Analytical approach is faster investigation method as compared to the latter ones for the parametric study. The analytical equations for determining the magnetic field [9–14], force and stiffness [15–22] in bearings with axial, radial and perpendicular polarizations are presented by the many researchers recently. However in these works, the ring magnets are concentric, which might not be prevailing in actual scenario. Secondly, the analytical expressions involve elliptical integrals or special functions which are tedious to deal with. The mathematical model of an axially magnetized permanent magnet bearing for force, stiffness and moment using Coulombian model and simple vector approach is presented by Bekinal et al. [23, 24]. The present work focuses on the mathematical treatment for evaluating force, moment and stiffness characteristics of a radial magnetized permanent magnet bearing considering three translational (x , y and z) degrees of freedom of the rotor magnet ring using a simple vector approach. A MATLAB code is written for estimating the forces, moments, stiffness and cross coupled stiffnesses between the stator-rotor made of two non-concentric ring magnets and also for multiple rings based on the Coulombian model and vector approach. The results of mathematical model are compared with the results of 3D FEA using ANSYS and a case available in the literature [25]. Finally, a 3×3 stiffness matrix (Eq. (1)) representing three degrees of freedom is developed for the elementary structure of the bearing and for stacked structure with three ring permanent magnets with alternate radial polarizations.

$$K = \begin{bmatrix} K_{XX} & K_{XY} & K_{XZ} \\ K_{YX} & K_{YY} & K_{YZ} \\ K_{ZX} & K_{ZY} & K_{ZZ} \end{bmatrix} \quad (1)$$

2. MATHEMATICAL MODELING

To estimate the bearing characteristics, the forces between two ring magnets, one fixed to the rotor and the other to the stator, need to be calculated. Two different approaches, namely, Lorentzian [16–18] and Coulombian [20–25] are available to determine the forces. In former approach the permanent magnet is considered as planes with equivalent currents, while the equivalent charge density in the later one. In the present analysis, equivalent charge density (Coulombian) is used with simple vector approach. In this approach, the permanent magnet is represented by surfaces with fictitious magnetic pole surface densities in the direction of polarization. The forces of attraction or repulsion between the polarized surfaces of the magnets are calculated using the Coulomb's law of force. The basic configuration of a permanent magnet bearing with radial polarized rings is presented in Fig. 1.

The inner magnet movement is considered in x , y and z directions with respect to the outer magnet. The inner and outer radii of the inner permanent magnet ring are $R1$ and $R2$ respectively and $R3$ and $R4$ are of outer permanent magnet ring. The thicknesses of the outer and inner magnets are $Z1 - Z0 = L$ and $Z3 - Z2 = L$ respectively. Magnetic polarization ' J ' of both the magnets is in the radial direction as depicted by Fig. 1. Modeling of the bearing is carried out by knowing the forces acting on the rotor magnet which in turn can be utilized to estimate the bearing stiffness. Fig. 2 shows the arrangement of rotor and stator magnets with magnetization in the radial directions. Surfaces A and C are the fictitious charged surfaces of rotor magnet

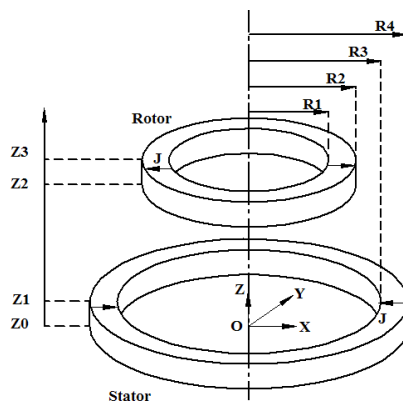


Figure 1. Configuration of a permanent magnet bearing with radial polarizations.

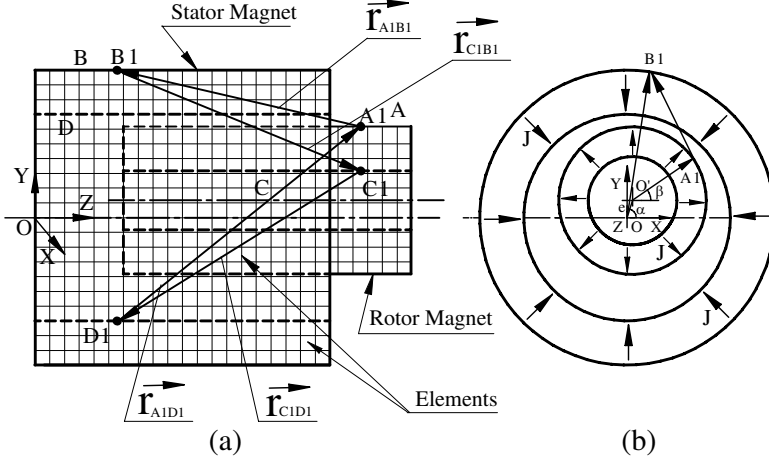


Figure 2. Arrangement of rotor and stator magnets. (a) Elements on the surfaces. (b) Displacement of the rotor magnet by a distance ‘e’ with respect to outer magnet.

and surfaces B and D are of stator magnet. There are magnetic forces of attraction and repulsion between the charged surfaces of the rotor and stator magnet. The net force acting is the bearing reactions for various positions of the rotor. The rotor magnet is displaced from its nominal position by a distance ‘e’ in XYZ coordinate system as shown in Fig. 2(b) and elements on the surfaces of the rotor and stator magnets in Fig. 2(a).

The elemental force on discrete surface element ‘A1’ of the rotor magnet surface ‘A’ due to the surface element ‘B1’ on the stator magnet surface ‘B’ can be expressed as [26]:

$$\vec{F}_{A1B1} = \frac{J^2 S_{A1} S_{B1}}{4\pi\mu_0 r_{A1B1}^3} \vec{r}_{A1B1} \quad (2)$$

where J is the magnet surface flux density (equal for both the magnets), S_{A1} the surface area of element A1, S_{B1} the surface area of element B1, \vec{r}_{A1B1} the distance vector between elements A1 and B1, and μ_0 the absolute magnetic permeability. The vector \vec{r}_{A1B1} can be expressed in XYZ coordinate system as:

$$\vec{r}_{A1B1} = (X_{B1} - X_{A1}) \mathbf{i} + (Y_{B1} - Y_{A1}) \mathbf{j} + (Z_{B1} - Z_{A1}) \mathbf{k} \quad (3)$$

where \mathbf{i} , \mathbf{j} and \mathbf{k} are the unit vectors in X , Y and Z axes, X_{A1} , Y_{A1} , Z_{A1} the coordinate of element A1, and X_{B1} , Y_{B1} , Z_{B1} the coordinate of the element B1. The coordinates of the discrete elements are expressed

by considering the movement of the rotor magnet $e = x\mathbf{i} + y\mathbf{j} + z\mathbf{k}$. The positions of the elements $A1$ and $B1$ in terms of radius, mean distance from the respective centers and the angles α, β are expressed as (Fig. 2(b)):

$$\begin{aligned}\vec{X}_{A1} &= (x + R2 \cos(\beta))\mathbf{i} & \vec{X}_{B1} &= (R4 \cos(\alpha))\mathbf{i} \\ \vec{Y}_{A1} &= (y + R2 \sin(\beta))\mathbf{j} & \vec{Y}_{B1} &= (R4 \sin(\alpha))\mathbf{j} \\ \vec{Z}_{A1} &= (z + L_{A1M})\mathbf{k} & \vec{Z}_{B1} &= (L_{B1M})\mathbf{k}\end{aligned}\quad (4)$$

where L_{A1M} is the mean axial distance (parallel to Z axis) of the element $A1$ from inner magnet centre ‘ O ’ and L_{B1M} the mean axial distance (parallel to Z axis) of element $B1$ from outer magnet centre ‘ O ’. Combining Eqs. (2) and (3), the elemental force in terms of components in the XYZ coordinate system can be written as:

$$\vec{F}_{A1B1} = F_{A1B1X}\mathbf{i} + F_{A1B1Y}\mathbf{j} + F_{A1B1Z}\mathbf{k}. \quad (5)$$

Similarly, elemental forces \vec{F}_{A1D1} , \vec{F}_{C1B1} and \vec{F}_{C1D1} due to elements on the rotor and stator magnet surfaces A, B, C and D can be written by considering the respective vector distances (Fig. 2(a)) as follows (Eqs. (6)–(12)):

$$\vec{r}_{A1D1} = (X_{A1} - X_{D1})\mathbf{i} + (Y_{A1} - Y_{D1})\mathbf{j} + (Z_{A1} - Z_{D1})\mathbf{k} \quad (6)$$

$$\vec{r}_{C1B1} = (X_{C1} - X_{B1})\mathbf{i} + (Y_{C1} - Y_{B1})\mathbf{j} + (Z_{C1} - Z_{B1})\mathbf{k} \quad (7)$$

$$\vec{r}_{C1D1} = (X_{D1} - X_{C1})\mathbf{i} + (Y_{D1} - Y_{C1})\mathbf{j} + (Z_{D1} - Z_{C1})\mathbf{k} \quad (8)$$

where X_{C1}, Y_{C1}, Z_{C1} is the coordinate of element $C1$ and X_{D1}, Y_{D1}, Z_{D1} is the coordinate of the element $D1$. The positions of the elements $C1$ and $D1$ in terms of radius, mean distance from the respective centers and angles α, β (Fig. 2(b)) can be written as:

$$\begin{aligned}\vec{X}_{C1} &= (x + R1 \cos(\beta))\mathbf{i} & \vec{X}_{D1} &= (R3 \cos(\alpha))\mathbf{i} \\ \vec{Y}_{C1} &= (y + R1 \sin(\beta))\mathbf{j} & \vec{Y}_{D1} &= (R3 \sin(\alpha))\mathbf{j}\end{aligned}\quad (9)$$

$$\vec{Z}_{C1} = (z + L_{C1M})\mathbf{k} \quad \vec{Z}_{D1} = (L_{D1M})\mathbf{k}$$

$$\vec{F}_{A1D1} = F_{A1D1X}\mathbf{i} + F_{A1D1Y}\mathbf{j} + F_{A1D1Z}\mathbf{k} \quad (10)$$

$$\vec{F}_{C1B1} = F_{C1B1X}\mathbf{i} + F_{C1B1Y}\mathbf{j} + F_{C1B1Z}\mathbf{k} \quad (11)$$

$$\vec{F}_{C1D1} = F_{C1D1X}\mathbf{i} + F_{C1D1Y}\mathbf{j} + F_{C1D1Z}\mathbf{k}. \quad (12)$$

Considering ‘ n ’ number of discrete elements on inner magnet surfaces and ‘ m ’ number of discrete elements on outer magnet surfaces, the resultant forces in X, Y and Z axes, on the rotor magnet can be expressed as a summation of all the elemental forces which are

presented below (Eqs. (13)–(15)):

$$F_X = \sum_{p=1, q=1}^{p=n, q=m} F_{ApBqX} + \sum_{p=1, q=1}^{p=n, q=m} F_{ApDqX} + \sum_{p=1, q=1}^{p=n, q=m} F_{CpBqX} + \sum_{p=1, q=1}^{p=n, q=m} F_{CpDqX} \quad (13)$$

$$F_Y = \sum_{p=1, q=1}^{p=n, q=m} F_{ApBqY} + \sum_{p=1, q=1}^{p=n, q=m} F_{ApDqY} + \sum_{p=1, q=1}^{p=n, q=m} F_{CpBqY} + \sum_{p=1, q=1}^{p=n, q=m} F_{CpDqY} \quad (14)$$

$$F_Z = \sum_{p=1, q=1}^{p=n, q=m} F_{ApBqZ} + \sum_{p=1, q=1}^{p=n, q=m} F_{ApDqZ} + \sum_{p=1, q=1}^{p=n, q=m} F_{CpBqZ} + \sum_{p=1, q=1}^{p=n, q=m} F_{CpDqZ}. \quad (15)$$

The stiffness of the bearing in Cartesian coordinate system is obtained by the method of numerical differentiation after evaluation of resultant forces. A three-point midpoint formula for differentiation is used to obtain stiffness values in radial and axial directions. In general, a three-point midpoint formula can be written as:

$$f'(X_0) = \frac{1}{2h} [f(X_0 + h) - f(X_0 - h)] - \frac{h^2}{6} f^{(3)}(\xi_1) \quad (16)$$

where ξ_1 lies between $(X_0 - h)$ and $(X_0 + h)$. It is assumed that data points are equally spaced along the X -axis such that $X_{i+1} - X_i = h$, a constant for $i = 0, 1, 2, \dots, n - 1$.

The principal radial stiffness exerted between two ring permanent magnets along X direction at x can be expressed as follows:

$$K_{XX} = \frac{dF_X}{dX} = \frac{1}{2\Delta x} [F_X(x + \Delta x) - F_X(x - \Delta x)] - \frac{\Delta x^2}{6} F_X^{(3)}(\xi) \quad (17)$$

where ξ lies between $(x - \Delta x)$ and $(x + \Delta x)$ and for smaller values of Δx , the Eq. (17) can be expressed as:

$$K_{XX} \cong \frac{dF_X}{dX} = \frac{1}{2\Delta x} [F_X(x + \Delta x) - F_X(x - \Delta x)]. \quad (18)$$

Similarly, principal radial stiffness along Y and principal axial stiffness in Z direction can be written as follows (Eqs. (19) and (20)):

$$K_{YY} \cong \frac{dF_Y}{dY} = \frac{1}{2\Delta y} [F_Y(y + \Delta y) - F_Y(y - \Delta y)] \quad (19)$$

$$K_{ZZ} \cong \frac{dF_Z}{dZ} = \frac{1}{2\Delta z} [F_Z(z + \Delta z) - F_Z(z - \Delta z)]. \quad (20)$$

Cross coupled radial and axial-radial stiffnesses can be expressed as (Eqs. (21)–(23)):

$$K_{XY} = K_{YX} \cong \frac{dF_X}{dY} = \frac{1}{2 \Delta y} [F_X(x + \Delta x) - F_X(x - \Delta x)] \quad (21)$$

$$K_{XZ} = K_{ZX} \cong \frac{dF_X}{dZ} = \frac{1}{2 \Delta z} [F_X(x + \Delta x) - F_X(x - \Delta x)] \quad (22)$$

$$K_{YZ} = K_{ZY} \cong \frac{dF_Z}{dY} = \frac{1}{2 \Delta y} [F_Z(z + \Delta z) - F_Z(z - \Delta z)]. \quad (23)$$

To determine the stiffness values in axial and radial directions in the presented model, the selected step sizes of x , y and z are $\Delta x = 0.05$ mm, $\Delta y = 0.05$ mm and $\Delta z = 0.5$ mm.

In practical cases, the rotor magnet movement can be assumed as a rigid body movement, estimation of the moment of the forces acting on the rotor magnet about its centre of gravity (geometric centre for axisymmetric and isotropic magnets) provides useful information about the dynamics of the rotor magnet. The moment due to elemental force \vec{F}_{A1B1} about the centre of gravity of the inner magnet can be written as:

$$\begin{aligned} M_{A1B1X} &= -F_{A1B1Y} \times \left(L_{A1M} - \frac{L}{2} \right) + F_{A1B1Z} \times R2 \sin(\beta) \\ M_{A1B1Y} &= F_{A1B1X} \times \left(L_{A1M} - \frac{L}{2} \right) - F_{A1B1Z} \times R2 \cos(\beta) \\ M_{A1B1Z} &= -F_{A1B1X} \times R2 \sin(\beta) + F_{A1B1Y} \times R2 \cos(\beta). \end{aligned} \quad (24)$$

Similarly, the moments due to elemental forces \vec{F}_{A1D1} , \vec{F}_{C1B1} and \vec{F}_{C1D1} about the centre of gravity of the rotor magnet can be written by following the proper sign convention as follows (Eqs. (25)–(27)):

$$\begin{aligned} M_{A1D1X} &= -F_{A1D1Y} \times \left(L_{A1M} - \frac{L}{2} \right) + F_{A1D1Z} \times R2 \sin(\beta) \\ M_{A1D1Y} &= F_{A1D1X} \times \left(L_{A1M} - \frac{L}{2} \right) - F_{A1D1Z} \times R2 \cos(\beta) \\ M_{A1D1Z} &= -F_{A1D1X} \times R2 \sin(\beta) + F_{A1D1Y} \times R2 \cos(\beta) \end{aligned} \quad (25)$$

$$\begin{aligned}
M_{C1B1X} &= -F_{C1B1Y} \times \left(L_{C1M} - \frac{L}{2} \right) + F_{C1B1Z} \times R1 \sin(\beta) \\
M_{C1B1Y} &= F_{C1B1X} \times \left(L_{C1M} - \frac{L}{2} \right) - F_{C1B1Z} \times R1 \cos(\beta) \quad (26)
\end{aligned}$$

$$\begin{aligned}
M_{C1B1Z} &= -F_{C1B1X} \times R1 \sin(\beta) + F_{C1B1Y} \times R1 \cos(\beta) \\
M_{C1D1X} &= -F_{C1D1Y} \times \left(L_{C1M} - \frac{L}{2} \right) + F_{C1D1Z} \times R1 \sin(\beta) \\
M_{C1D1Y} &= F_{C1D1X} \times \left(L_{C1M} - \frac{L}{2} \right) - F_{C1D1Z} \times R1 \cos(\beta) \quad (27) \\
M_{C1D1Z} &= -F_{C1D1X} \times R1 \sin(\beta) + F_{C1D1Y} \times R1 \cos(\beta).
\end{aligned}$$

The net moment acting on the rotor magnet is expressed using Eqs. ((24)–(27)) as:

$$\begin{aligned}
M_X &= \sum_{p=1, q=1}^{p=n, q=m} M_{ApBqX} + \sum_{p=1, q=1}^{p=n, q=m} M_{ApDqX} \\
&\quad + \sum_{p=1, q=1}^{p=n, q=m} M_{CpBqX} + \sum_{p=1, q=1}^{p=n, q=m} M_{CpDqX} \quad (28)
\end{aligned}$$

$$\begin{aligned}
M_Y &= \sum_{p=1, q=1}^{p=n, q=m} M_{ApBqY} + \sum_{p=1, q=1}^{p=n, q=m} M_{ApDqY} \\
&\quad + \sum_{p=1, q=1}^{p=n, q=m} M_{CpBqY} + \sum_{p=1, q=1}^{p=n, q=m} M_{CpDqY} \quad (29)
\end{aligned}$$

$$\begin{aligned}
M_Z &= \sum_{p=1, q=1}^{p=n, q=m} M_{ApBqZ} + \sum_{p=1, q=1}^{p=n, q=m} M_{ApDqZ} \\
&\quad + \sum_{p=1, q=1}^{p=n, q=m} M_{CpBqZ} + \sum_{p=1, q=1}^{p=n, q=m} M_{CpDqZ}. \quad (30)
\end{aligned}$$

The forces and moment acting on the rotor magnet as well as the radial and axial stiffness of the bearing are calculated and presented in the following section. This mathematical model can be used for different configurations of permanent magnet bearings made of radial magnetized rings.

3. VALIDATION OF PROPOSED MODEL

The proposed mathematical model is used to determine the axial force and stiffness values of permanent magnet bearing made of two concentric rings with radial polarizations as presented earlier (Fig. 1). Geometrical parameters considered for the analysis are given in Table 1.

This configuration produces positive radial stiffness; however, axial stiffness becomes negative. The axial force and stiffness values

along with the results of [25] are shown in Fig. 3. The mathematical model of the configuration converges at a particular number of elements on stator as well as on rotor magnet faces and convergence results of the model are presented in Table 2. Comparison of the results of the

Table 1. Dimensions of the configuration.

	Inner ring dimensions	Outer ring dimensions
Inner radius [mm]	$R1 = 10$	$R3 = 22$
Outer radius [mm]	$R2 = 20$	$R4 = 32$
Thickness, L [mm]	$Z1 - Z0 = 10$	$Z3 - Z2 = 10$
Flux density [T]	$J1 = 1$	$J2 = 1$

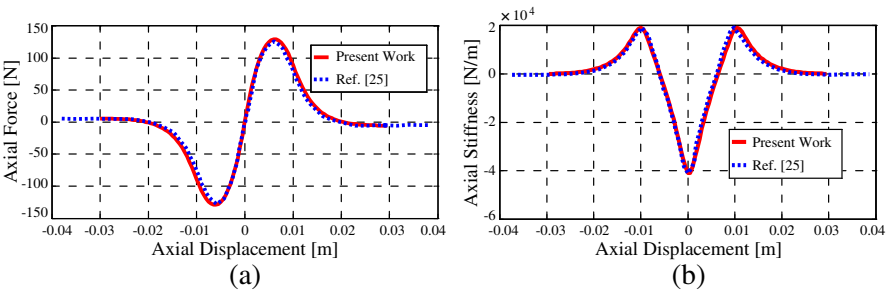


Figure 3. Characteristics of permanent magnet bearing made of two concentric rings with radial polarizations. (a) Axial Force. (b) Axial Stiffness.

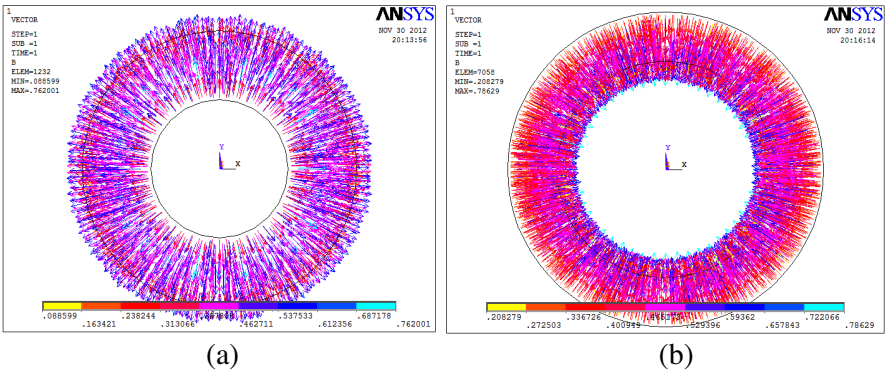


Figure 4. Finite element model in ANSYS. (a) Inner ring magnet with radially outward magnetization. (b) Outer ring magnet with radially inward magnetization.

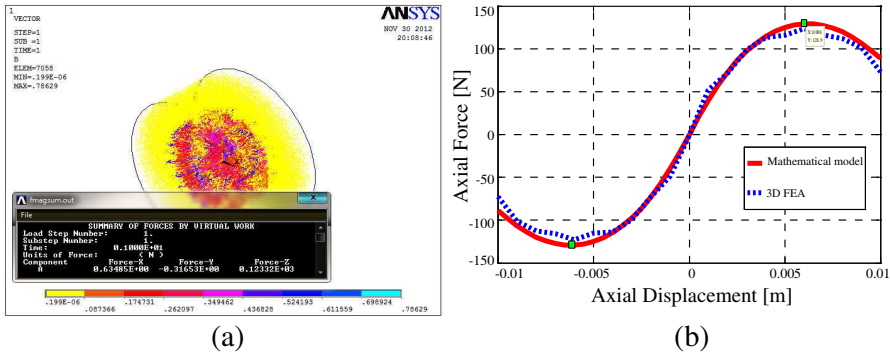


Figure 5. Results of finite element analysis. (a) Maximum force exerted on the inner ring. (b) Axial force comparison.

Table 2. Convergence results of mathematical model of the configuration with radial polarizations.

Number of elements on the stator and the rotor magnet faces	Axial Force [N]	Axial Stiffness $ K_Z $ [N/m]
$m = n = 144 \times 2$	172.52	161940
$m = n = 144 \times 5 = 720$	130.93	47472
$m = n = 216 \times 5 = 1080$	130.93	47471
$m = n = 144 \times 10 = 1440$	128.93	40986
$m = n = 216 \times 10 = 2160$	128.94	40735
$m = n = 288 \times 10 = 2880$	128.94	40723
$m = n = 432 \times 10 = 4320$	128.94	40722

Table 3. Comparison of results of configuration with radial polarizations.

	Results of present work	Results of Ravaud and Lemarquand [25]	Variation [%]
Axial Force [N]	128.94	126.3	2.09
Axial Stiffness $ K_Z $ [N/m]	40722	40282	1.09

proposed model with that reported in Ravaud and Lemarquand [25] is presented in Table 3.

The results of Fig. 3 and Table 3 demonstrate that the evaluated

axial force and stiffness values match very closely with that of reported analytical results for the same bearing configuration. A finite element model of the bearing with radially magnetized rings was created in ANSYS and the model is analysed with 220283 solid 97 elements and 39414 nodes (Fig. 4). The properties of the magnetic material considered for the analysis are: $B_r = 1.05$ T, $H_c = 796$ kA/m and $\mu_r = 1.049$. The magnetic virtual displacement approach is used to determine the force (bearing load) acting on the inner ring (Fig. 5(a)). The force exerted by the stator ring on the rotor is plotted for its different axial positions in Fig. 5(b).

Figure 5 shows that the results of axial force obtained with 3D FEA match closely with the results of mathematical model with same optimal points. The mismatch between the results is less than 5%. The MATLAB code of the model involves the calculation of forces, moments, radial and axial stiffnesses at one stretch. So the computational cost of the code is 11.5 s for a bearing made of two ring permanent magnets for one iteration which is significantly lower as compared to evaluating the parameters using finite element analysis tools like ANSYS, COMSOL, MAXWELL 3D, etc.

4. ANALYSIS OF RADIAL MAGNETIZED BEARING CONFIGURATIONS

4.1. Elementary Structure

The elementary configuration, shown in Fig. 6 is analysed for force, moment and stiffness parameters. The configuration is suitable for radial bearing application developing positive radial stiffness having negative axial stiffness.

The axial force and stiffness values are calculated as a function

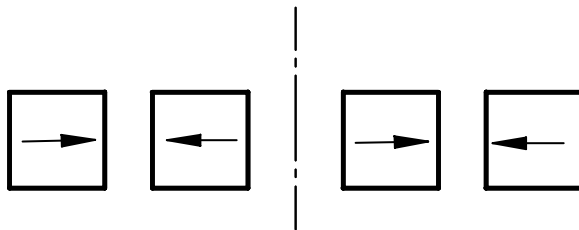


Figure 6. Cross-section view of two ring permanent magnet configuration with radial polarizations: $R1 = 20$ mm, $R2 = 30$ mm, $R3 = 32$ mm, $R4 = 42$ mm, $Z1 - Z0 = 10$ mm, $Z3 - Z2 = 10$ mm, $J = 1.2$ T.

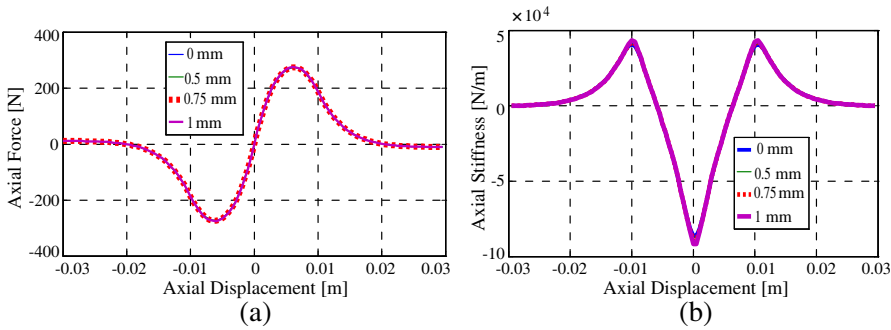


Figure 7. Characteristics of configuration. (a) Axial force. (b) Axial stiffness.

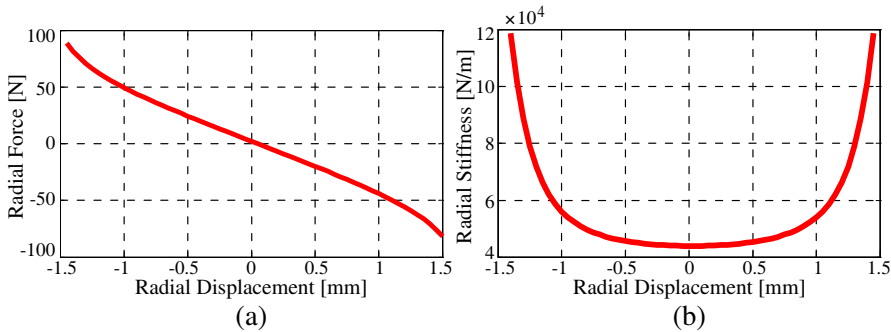


Figure 8. Characteristics of configuration. (a) Radial force. (b) Radial stiffness.

Table 4. Results of characteristics of a permanent magnet bearing with radial polarizations (Fig. 6).

Radial offset [mm]	0	0.5	0.75	1
Maximum axial force [N]	271.7	272.5	273.4	274.7
Maximum axial stiffness $ K_Z $ [N/m]	86115	87380	89094	91800
Maximum moment about Y axis [Nm]	0	0.047	0.071	0.095

of radial offset values (0.5, 0.75 and 1 mm) of the rotor magnet in the positive X direction for various axial positions of the rotor magnet for the configuration (Fig. 6) and the results are presented in Fig. 7. The radial force and stiffness values of the bearing configuration are calculated as a function of radial displacement and are results are presented in Fig. 8.

The moments acting on the rotor magnet as a result of radial

displacements (0.5, 0.75 and 1 mm) are calculated as a function of various axial positions of the rotor for the elementary configuration and results are plotted in Fig. 9.

The maximum axial force exerted by the outer ring on the inner one, the maximum axial stiffness $|K_Z|$ and maximum moment about Y -axis in the configuration are presented in Table 4.

Calculations shown in Table 4 demonstrate that the radial displacement of the rotor in X -axis generates moment about the Y -axis of the rotor magnet and vice-versa. The resultant moment about the Z -axis of the rotor magnet are zero. The magnitudes of moments increase with the higher radial offset value and they diminish when the inner magnet is concentric with the outer magnet. The influence of radial offset on the axial force and stiffness values is least, whereas on the moment is quite prominent. A 3×3 stiffness matrix at an axial offset of 3 mm for the configuration (Fig. 6) is presented in Table 5. No cross coupling of stiffnesses between X and Y axes is observed from the analysis.

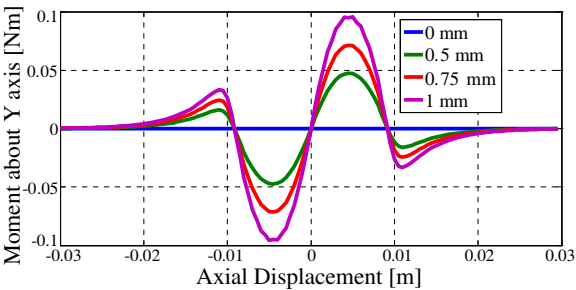


Figure 9. Moment about Y -axis at various radial displacements in X -axis.

Table 5. Stiffness matrix of a permanent magnet bearing with radial polarizations (Fig. 6).

	X	Y
X	23.91 N/mm	0
Y	0	23.91 N/mm
Z	−3.83 N/mm at $x = 0.5$ mm	−3.83 N/mm at $y = 0.5$ mm
	−7.61 N/mm at $x = 1.0$ mm	−7.61 N/mm at $y = 1.0$ mm
	−9.07 N/mm at $x = 1.5$ mm	−9.07 N/mm at $y = 1.5$ mm

	Z
X	$-3.83 \text{ N/mm at } x = 0.5 \text{ mm}$
	$-7.61 \text{ N/mm at } x = 1.0 \text{ mm}$
	$-9.07 \text{ N/mm at } x = 1.5 \text{ mm}$
Y	$-3.83 \text{ N/mm at } y = 0.5 \text{ mm}$
	$-7.61 \text{ N/mm at } y = 1.0 \text{ mm}$
	$-9.07 \text{ N/mm at } y = 1.5 \text{ mm}$
Z	-47.82 N/mm

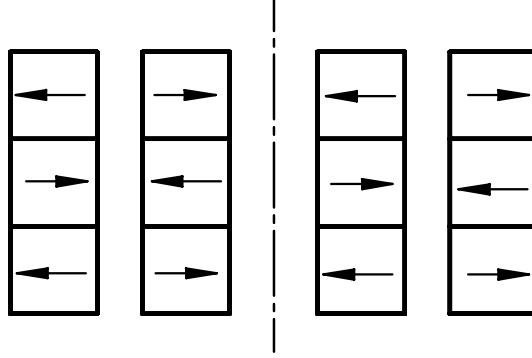


Figure 10. Cross-section view of a permanent magnet bearing composed of three ring pairs with alternate radial polarizations: $R1 = 20 \text{ mm}$, $R2 = 30 \text{ mm}$, $R3 = 32 \text{ mm}$, $R4 = 42 \text{ mm}$, $J = 1.2 \text{ T}$, the height of each permanent magnet ring = 10 mm .

4.2. Stacked Structure with Three Ring Permanent Magnets

The configuration composed of three ring pairs with alternate radial polarizations is presented in Fig. 10. The variations of axial force and stiffness of the configuration with radial offset for different axial positions of the rotor are depicted by Fig. 11.

The radial force and stiffness values of the bearing configuration are calculated as a function of radial displacement and are presented in Fig. 12. The results show that the radial force increases linearly with radial offset, whereas radial stiffness is constant up to a particular value of radial offset (1 mm) and then increases suddenly.

The moments acting on the rotor magnets as the result of radial displacements in configuration (Fig. 10) are plotted in Fig. 13. The proposed mathematical approach for the configuration presented in Fig. 10 leads to results listed in Table 6.

Results shown in Table 6 demonstrate that the magnitudes of

moments increase with the higher radial offset value and they diminish when the inner magnet is concentric with the outer magnet. A 3×3 stiffness matrix at an axial offset of 3.0 mm for the configuration shown

Table 6. Results of configuration of permanent magnet bearing made of three ring pairs with alternate radial polarizations (Fig. 10).

Radial offset [mm]	0	0.5	0.75	1
Maximum axial force [N]	1181.25	1185.95	1191.84	1200.16
Maximum axial stiffness $ K_Z $ [N/m]	411840	419028	429018	445336
Maximum moment about Y axis [Nm]	0	0.37	0.56	0.75

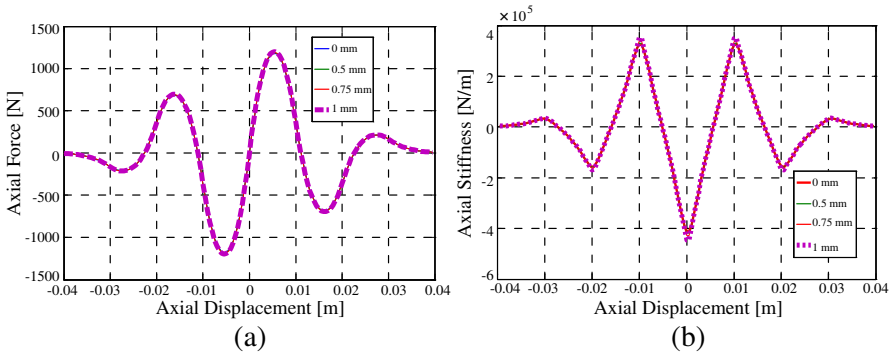


Figure 11. Characteristics of permanent magnet bearing made of three ring pairs with alternate radial polarizations. (a) Axial force. (b) Axial Stiffness.

Table 7. Stiffness matrix of the configuration (Fig. 10).

	X	Y
X	106.15 N/mm	0
Y	0	106.15 N/mm
Z	-20.58 N/mm at $x = 0.5$ mm -40.87 N/mm at $x = 1.0$ mm -49.49 N/mm at $x = 1.5$ mm	-20.58 N/mm at $y = 0.5$ mm -40.87 N/mm at $y = 1.0$ mm -49.49 N/mm at $y = 1.5$ mm

	Z
X	-20.58 N/mm at $x = 0.5 \text{ mm}$
	-40.87 N/mm at $x = 1.0 \text{ mm}$
	-49.49 N/mm at $x = 1.5 \text{ mm}$
Y	-20.58 N/mm at $y = 0.5 \text{ mm}$
	-40.87 N/mm at $y = 1.0 \text{ mm}$
	-49.49 N/mm at $y = 1.5 \text{ mm}$
Z	-212.31 N/mm

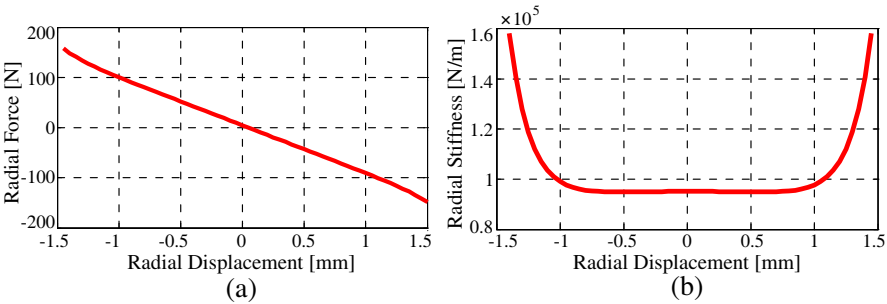


Figure 12. Characteristics of permanent magnet bearing made of three ring pairs with alternate radial polarizations. (a) Radial force. (b) Radial Stiffness.

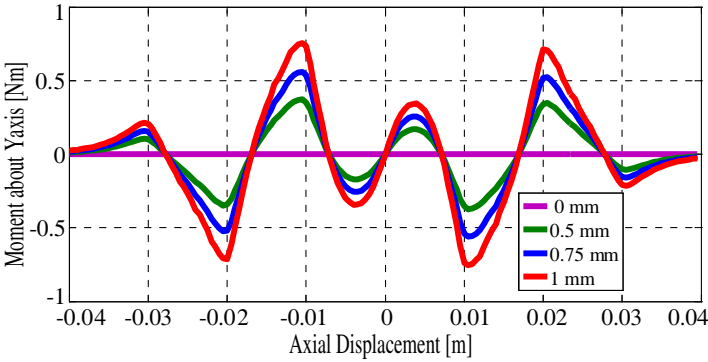


Figure 13. Moment about Y-axis at various radial displacements in X-axis.

in Fig. 10 is presented in Table 7. No cross coupling of stiffnesses between X and Y axes is observed from the analysis.

5. CONCLUSIONS

A simple mathematical model employing the Coulombian model using a vector approach is presented for the investigation of force, moment on the rotor and stiffness of a permanent magnet bearing made of rings with radial polarizations. Comparison of the results of mathematical model of radial magnetized permanent magnet bearings with the results of 3D FEA shows good agreement. An attempt has been made to determine the effect of radial and axial displacements of the rotor on force, stiffness and moment in permanent magnet bearings. The effect of radial displacement on force and stiffness is least, whereas on the moment is quite prominent (magnitude of moment about X or Y -axis increases with the higher radial offset value). The magnitude of moment increases with an increase in the number of rings in the stack. The characteristics of the permanent magnet bearing are presented by calculating 3×3 stiffness matrix representing three degrees of freedom. The presented work can be used for optimizing the design of the radial magnetized permanent magnet bearings for a wide variety of applications and also, this method involves less computation than the approaches utilizing elliptical integrals.

REFERENCES

1. Yonnet, J. P., "Passive magnetic bearings with permanent magnets," *IEEE Trans. Magn.*, Vol. 14, No. 5, 803–805, 1978.
2. Yonnet, J. P., "Permanent magnetic bearings and couplings," *IEEE Trans. Magn.*, Vol. 17, No. 1, 1169–1173, 1981.
3. Delamare, J., E. Rulliere, and J. P. Yonnet, "Classification and synthesis of permanent magnet bearing configurations," *IEEE Trans. Magn.*, Vol. 31, No. 6, 4190–4192, 1995.
4. Chu, H. Y., Y. Fan, and C. S. Zhang, "A novel design for the flywheel energy storage system," *Proceedings of the Eighth International Conference on Electrical Machines and Systems*, Vol. 2, 1583–1587, 2005.
5. Guilherme, G. S., R. Andrade, and A. C. Ferreira, "Magnetic bearing sets for a flywheel system," *IEEE Trans. on Applied Super Conductivity*, Vol. 17, No. 2, 2150–2153, 2007.
6. Hussien, A., et al., "Application of the repulsive-type magnetic bearing for manufacturing micromass measurement balance

- equipment,” *IEEE Trans. Magn.*, Vol. 41, No. 10, 3802–3804, 2005.
7. Ohji, T., et al., “Conveyance test by oscillation and rotation to a permanent magnet repulsive-type conveyor,” *IEEE Trans. Magn.*, Vol. 40, No. 4, 3057–3059, 2004.
 8. Yonnet, J. P., et al., “Stacked structures of passive magnetic bearings,” *J. Appl. Phys.*, Vol. 70, No. 10, 6633–6635, 1991.
 9. Ravaud, R., G. Lemarquand, and R. Lemarquand, “Analytical calculation of the magnetic field created by permanent magnet rings,” *IEEE Trans. Magn.*, Vol. 44, No. 8, 1982–1989, 2008.
 10. Ravaud, R. and G. Lemarquand, “Comparison of the coulombian and amperian current models for calculating the magnetic field produced by radially magnetized arc shaped permanent magnets,” *Progress In Electromagnetics Research*, Vol. 95, 309–327, 2009.
 11. Ravaud, R., G. Lemarquand, V. Lemarquand, and C. Depollier, “Discussion about the analytical calculation of the magnetic field created by permanent magnets,” *Progress In Electromagnetics Research B*, Vol. 11, 281–297, 2009.
 12. Babic, S. I. and C. Akyel, “Improvement in the analytical calculation of the magnetic field produced by permanent magnet rings,” *Progress In Electromagnetics Research C*, Vol. 5, 71–82, 2008.
 13. Selvaggi, J. P., et al., “Calculating the external magnetic field from permanent magnets in permanent-magnet motors — An alternative method,” *IEEE Trans. Magn.*, Vol. 40, No. 5, 3278–3285, 2004.
 14. Ravaud, R., G. Lemarquand, and V. Lemarquand, “Magnetic field created by tile permanent magnets,” *IEEE Trans. Magn.*, Vol. 45, No. 7, 2920–2926, 2009.
 15. Azukizawa, T., S. Yamamoto, and N. Matsuo, “Feasibility study of a passive magnetic bearing using the ring shaped permanent magnets,” *IEEE Trans. Magn.*, Vol. 44, No. 11, 4277–4280, 2008.
 16. Paden, B., N. Groom, and J. Antaki, “Design formulas for permanent-magnet bearings,” *ASME Trans.*, Vol. 125, 734–739, 2003.
 17. Chen, C., et al., “A magnetic suspension theory and its application to the heart quest ventricular assist device,” *Artificial Organs*, Vol. 26, No. 11, 947–951, 2002.
 18. Yoo, S., et al., “Optimal design of non-contact thrust bearing using permanent magnet rings,” *International Journal of Precision Engineering and Manufacturing*, Vol. 12, No. 6, 1009–

- 1014, 2011.
19. Samanta, P. and H. Hirani, "Magnetic bearing configurations: Theoretical and experimental studies," *IEEE Trans. Magn.*, Vol. 44, No. 2, 292–300, 2008.
 20. Lang, M., "Fast calculation method for the forces and stiffnesses of permanent-magnet bearings," *8th International Symposium on Magnetic Bearing*, 533–537, 2002.
 21. Ravaut, R., G. Lemarquand, and V. Lemarquand, "Force and stiffness of passive magnetic bearings using permanent magnets. Part 1: Axial magnetization," *IEEE Trans. Magn.*, Vol. 45, No. 7, 2996–3002, 2009.
 22. Ravaut, R., G. Lemarquand, and V. Lemarquand, "Force and stiffness of passive magnetic bearings using permanent magnets. Part 2: Radial magnetization," *IEEE Trans. Magn.*, Vol. 45, No. 9, 3334–3342, 2009.
 23. Bekinal, S. I., T. R. Anil, and S. Jana, "Force, moment and stiffness characteristics of permanent magnet bearings," *Proceedings of National Symposium on Rotor Dynamics*, Indian Institute of Technology, Madras, India, 161–168, 2011.
 24. Bekinal, S. I., T. R. Anil, and S. Jana, "Analysis of axially magnetized permanent magnet bearing characteristics," *Progress In Electromagnetics Research B*, Vol. 44, 327–343, 2012.
 25. Ravaut, R. and G. Lemarquand, "Halbach structures for permanent magnets bearings," *Progress In Electromagnetics Research M*, Vol. 14, 263–277, 2010.
 26. Mukhopadhyaya, S. C., et al., "Fabrication of a repulsive-type magnetic bearing using a novel arrangement of permanent magnets for vertical-rotor suspension," *IEEE Trans. Magn.*, Vol. 39, No. 5, 3220–3222, 2003.